Novel Static Carrier Based Low Frequency Multilevel Modulations With Long Conduction Time : Analysis Of Capacitor Voltage Balancing

Corentin Darbas, Jean-Christophe Olivier, Nicolas Ginot, Frédéric Poitiers

Novel Static Carrier Based Low Frequency Multilevel Modulations With Long Conduction Time : Analysis Of Capacitor Voltage Balancing

Corentin Darbas
IETR UMR CNRS 6164
Université de Rennes 1 Campus Beaulieu, 263 ave. Général Leclerc,
CEDEX, 35042 Rennes, France
Corentin.Darbas@univ-nantes.fr

Jean-Christophe Olivier
IREENA
Université de Nantes, (CRTT), B.P. 406, 37 Bd de l'Université,
CEDEX, 44602 Saint-Nazaire, France
Jean-Christophe.Olivier@univ-nantes.fr

Nicolas Ginot
IETR UMR CNRS 6164
Université de Rennes 1 Campus Beaulieu, 263 ave. Général Leclerc,
CEDEX, 35042 Rennes, France
Nicolas.Ginot@univ-nantes.fr

Frédéric Poitiers
IETR UMR CNRS 6164
Université de Rennes 1 Campus Beaulieu, 263 ave. Général Leclerc,
CEDEX, 35042 Rennes, France
Frederic.Poitiers@univ-nantes.fr

***Abstract*— That work investigates the compatibility of voltage balancing algorithm and multilevel modulations of a three phase modular multilevel converter (MMC). A study of the "Reduced switching frequency" (RSF) voltage balancing algorithm with low frequency modulations is proposed. It is first shown that Nearest Level Modulation cannot be used in MMC with RSF algorithm. Two new hybrid modulations are then introduced, the Long Conduction time Pulse Width Modulation (LCPWM) and the Enhanced Long Conduction time Pulse Width Modulation (ELCPWM). They offer advantageous trade-off between switching frequency and voltage balancing accuracy with RSF algorithm. Based on innovative static carriers, they do not generate random narrow pulses, decreasing electrical stress on power transistors. The conduction times of the proposed modulations are deterministic and maximized. Their generation is highly simplified compared to triangular or saw-tooth carrier based modulations. An accurate simulation tool allows to compare various characteristics of proposed modulations to classical low frequency modulation and pulse width modulation on multi-megawatts three phase MMC.**

Keywords—power electronics, Modular Multilevel Converter (MMC), low frequency modulations, long conduction time modulations

I. INTRODUCTION (*HEADING 1*)

First introduced by Lesnicar and Marquard [1], the Modular Multilevel Converter (MMC) has become one of the most promising topology for high voltage applications like High-Voltage Direct Current (HVDC). Multilevel topologies exhibit low losses due to low switching frequency, allowing reduced stress on power modules and higher conversion efficiency. They offer superior power quality compared to two-level converters. The MMC is the first multilevel power converter which does not requires separated DC buses, and is fully modular and scalable. One MMC phase consists of two "arms" (Up and Low). Each arm is a chain of N smaller switching cells connected in series with an inductor L_{arm}. The three-phase MMC is pictured Fig. 1. The switching cells, or Submodules (SM), can be of various types [2][3]. In that work, the so-called "Half-Bridge Submodule" (HBSM) is studied. It offers low conduction losses and control simplicity. It is based on two switches T_1 and T_2 in a half bridge topology, and a capacitor C_{SM} charged to a voltage V_C. The HBSM is given Fig. 2. The SM capacitor is said inserted (submodule in ON state) when T_1 is closed ($V_{SM} = V_C$), and bypassed (submodule in OFF state) when T_2 is closed ($V_{SM} = 0$ V).

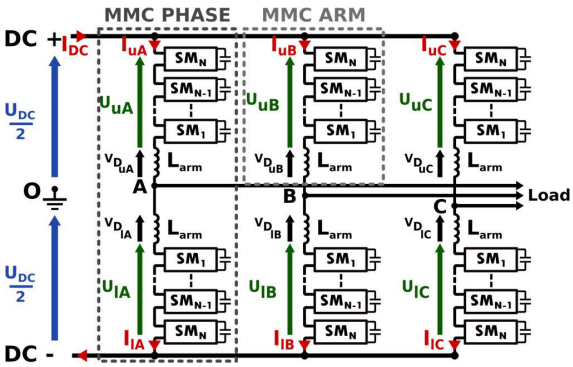

Fig. 1. Three phase Modular Multilevel Converter (MMC)

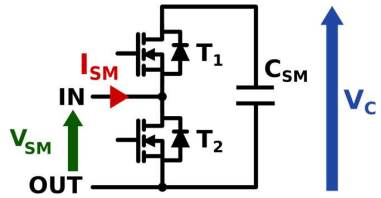

Fig. 2. MMC arm Half-Bridge Submodule (HBSM)

The converter model had been thoroughly studied in the past decades [4][5]. The three phase output voltages V_{outA}, V_{outB} and V_{outC} at points A, B and C can be of $N + 1$ levels or $2N + 1$ levels depending on the chosen modulation [6]. As seen on Fig. 1 (a), the output current of phase j is obtained by Kirchhoff's current law and expressed as in (1):

$$i_{outj} = i_{uj} - i_{lj} \quad (1)$$

The load current is a common mode current flowing from both DC side poles. All the differential mode current flowing from one pole to the other pole of the DC bus is called circulating current $I_{circ,j}$. It is not flowing in the load and must be regulated, as it generates losses. Furthermore, due to both

load and circulating currents, the arm capacitors voltages fluctuate. In most cases, a "Voltage Balancing Algorithm (VBA)" is used to maintain the arm capacitor voltages close together [7].

A wide variety of MMC control schemes had been proposed in the literature [8–11]. The different control structures can mostly be divided in two distinct categories. The first one is often called "decentralized control". A "master" controller is generally in charge of the regulation of the output quantities (voltages and/or currents) and the circulating currents, where p slave controllers are dedicated to a group of p submodules. These slave controllers can be in charge of various control tasks like capacitor voltage regulation or reference modulation [8][9]. Decentralized control is given Fig. 3. The other approach is the "centralized control". Only one main controller is in charge of the whole converter regulation. In some cases, the Voltage balancing algorithm is executed by the main controller [10]. However, when the number of submodule is high, the calculation burden can be heavy. An external voltage balancing algorithm can be used [11], usually executed by dedicated fast hardware like FPGA. In such cases, the modulation stage is in charge of the calculation of the "insertion index" $n_{i,j}$. $n_{i,j}$ is the number of inserted capacitor in the arm i of phase j. The VBA stage selects the appropriate $n_{i,j}$ capacitors to insert in each arm. The MMC with centralized control and external VBA is given Fig. 4. Various external VBA had been proposed in the literature [12–15]. They are independent on the multilevel modulation methods.

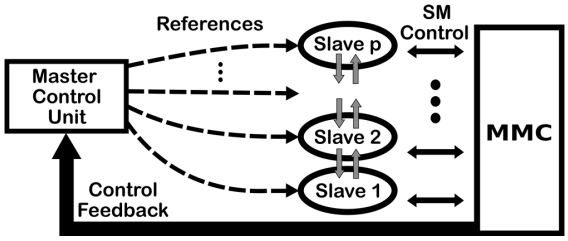

Fig. 3. Typical MMC decentralized control scheme

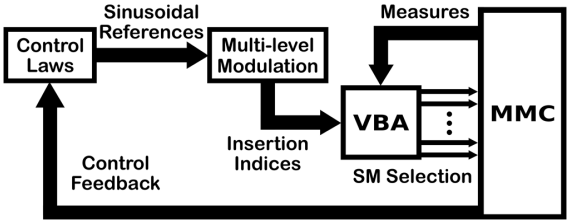

Fig. 4. Typical MMC centralized control scheme

That paper focuses on the algorithm presented in [15], named "Reduced Switching Frequency" (RSF) Voltage Balancing Algorithm. It shows through analysis and simulation the incompatibility of conventional nearest Level Modulation (NLM) and RSF algorithm. To solve that issue, that work introduces novel hybrid low frequency multilevel modulations with long and deterministic conduction times. They are generated with original static carriers, ensuring very low computational cost, while being compatible with RSF algorithm. The proposed modulations ensure longest possible conduction times, avoiding distortions of the output waveform due to so called "narrow pulses" generated by conventional carrier-based Pulse Width Modulations (PWM).

That paper is organized as follows. First, the incompatibility of RSF algorithm with Nearest Level Modulation is demonstrated. The NLM waveform is generated with static carriers. Secondly, two new modulation technics are introduced with modified static carriers: the Long Conduction Time Pulse Width Modulation (LCPWM) and the Enhanced Long Conduction Time Pulse Width Modulation (ELCPWM). There compatibility with RSF algorithm is demonstrated. There generation principle is based on maximizing the conduction times while limiting the number of switching. Finally, last section will demonstrate the feasibility of the proposed modulation schemes with a three-phase MMC simulation on Matlab/Simscape. It will allow to compare the different modulations introduced in that work with a typical multilevel PWM when used with RSF algorithm.

II. Nearest Level Modulation with Static Carriers and Study of RSF Compatibility

A. Static carriers for low frequency modulation

MMC modulation techniques can be mostly divided in two categories. The high frequency modulations, like Pulse Width Modulation, and the low frequency modulations like NLM. Conventional multilevel PWM is based on comparison of a reference with triangular or saw-tooth carriers. A wide variety of carrier space distribution had been studied in the literature [16]. An example of multilevel PWM called Phase-Disposition PWM (PDPWM) is presented Fig. 5 (a), with both multilevel carriers (Up) and output insertion index (Down). The output waveform exhibits high frequency behavior. NLM is generally obtained by discretization of the reference [17]. In that work, the reference is compared to "static carriers" in order to generate the desired waveform, as proposed in [18]. The NLM with static carriers is given Fig. 5. With low frequency modulations, "staircase" waveforms are generated.

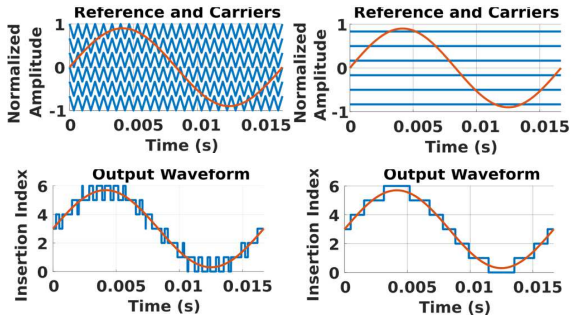

Fig. 5. PDPWM (a) and NLM (b) modulations

The PWM output power quality is generally superior than that of NLM. But the higher the number of submodules, the higher the number of output level, thus the better the quality of low frequency modulations. High frequency modulations generate higher switching losses than low frequency modulations. Compared to PWM, NLM has non-constant switching frequency. The instants of switching are imposed by the voltage reference derivative. Furthermore, conventional PWM generate narrow pulses that can damage the switching devices [19,20]. In many applications, an inherent delay exists between the command pulses and the actual switchings [21]. Such narrow pulses can thus lead to distortions of the output voltage waveform. For those reasons, low frequency

modulations are generally preferred in applications with high number of submodule. The generation of *6N* triangular carriers can occupy a lot of hardware resources. In contrast, static carriers are extremely simple to generate. The NLM generated with static carriers is thus very promising for converters with high number of submodules.

The space disposition of the static carriers proposed in that work follows a simple equation, making their generation by a numerical system straightforward. An equal repartition of the carriers is proposed, i.e, the space between each carrier is constant. Furthermore, no offset is added at the output waveform, as could be proposed in [6]. Thus, all carriers are symmetrical regarding the center of the modulation space. Here, the normalized space is studied. The normalized reference voltage $V_{ref_{norm}}$ takes its values between 1 and -1 as in (2).

$$-1 < V_{ref_{norm}} = \frac{V_{ref}}{U_{DC}/2} = m \sin(\omega t + \varphi) < 1 \qquad (2)$$

With m the modulation index defined by the ratio of the output voltage reference V_{ref} and its maximum value $U_{DC}/2$. The angular frequency reference is ω and the phase reference is φ. Having N carriers for an output voltage of $N + 1$ levels, each carrier can be numbered from 1 (closest to -1) to N (closest to 1). Each carrier p is associated to a line D_p which equation is given in (3). From that simple equation, the NLM can be generated, highly reducing the computational burden compared to triangular or saw-tooth carriers.

$$D_p = \frac{2}{N}(p-1) + \frac{1}{N} - 1 = \frac{2p-1}{N} - 1 \qquad (3)$$

The number of switchings per period N_{sw} can be easily determined for NLM with static carriers. Each time the reference crosses a carrier, a switching occurs. Thus, the number of switching per period equals $2N_{carr}$, where N_{carr} is the number of carrier between the reference maximum and minimum values, i.e. m and $-m$. N_{sw} is given in (3):

$$N_{carr} = 2p_{max} - N \qquad (4)$$

where p_{max} is the highest index carrier satisfying (5).

$$m < D_p = \frac{2p_{max} - 1}{N} - 1 \qquad (5)$$

Finally, the number of switching per period N_{sw} due to NLM with static carriers is given in (6), with $\lfloor x \rfloor$ the rounded down value of x.

$$N_{sw} = 4p_{max} - 2N$$

$$N_{sw} = 4\left\lfloor \left(\frac{N(m+1)+1}{2} \right) \right\rfloor - 2N \qquad (6)$$

B. Reduced Switching Frequency algorithm with Nearest Level Modulation

When RSF algorithm proposed in [15] is used, the number of switching occurring in the converter arm is strictly imposed by the modulation stage. It is not the case with other voltage balancing algorithms. The algorithm flowchart is given Fig. 6.

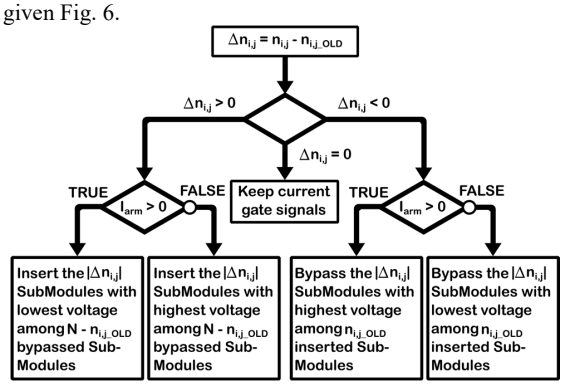

Fig. 6. RSF Flowchart [15]

The general scheme of voltage balancing algorithms is based on the generation of a list of submodule, with capacitor voltages in ascending or descending order, depending on the arm current sign. The inserted submodules are the $n_{i,j}$ first in the ascending list if the arm current is positive, and the $n_{i,j}$ first in the descending list otherwise. This leads to a voltage increase of the lowest charged capacitors, or a voltage decrease of the highest charged capacitors. A large variety of VBA had been proposed in the literature. However, such algorithms always lead to an increase in the switching frequency. With RSF algorithm, the number of switchings is limited to $\Delta n_{i,j}$, defined in (7), where n_{i,j_OLD} is the current insertion index and $n_{i,j}$ the desired insertion index.

$$\Delta n_{i,j} = n_{i,j} - n_{i,j\_OLD} \qquad (7)$$

When $\Delta n_{i,j} > 0$, only $\Delta n_{i,j}$ submodules among the bypassed submodules are switched ON. When $\Delta n_{i,j} < 0$, only $\Delta n_{i,j}$ submodules among the inserted submodules are switched OFF. Due to the staircase waveform of the NLM, the sign of Δn_{ij} is imposed by the reference derivative sign. There are only submodule insertions during one reference half-period, when the voltage reference is increasing. During the other half-period, there are only submodule bypassing, when the voltage reference is decreasing. This is sum up in equation (8) for a sine wave reference as in (2).

$$\begin{cases} \omega t \in \left[-\frac{\pi}{2}; \frac{\pi}{2}\right] \leftrightarrow \frac{dV_{ref}}{dt} > 0 \leftrightarrow \Delta n_{i,j} > 0 \\ \omega t \in \left[\frac{\pi}{2}; \frac{3\pi}{2}\right] \leftrightarrow \frac{dV_{ref}}{dt} < 0 \leftrightarrow \Delta n_{i,j} < 0 \end{cases} \qquad (8)$$

According to RSF algorithm flowchart and (8), the submodule selection process only depends on the arm current sign during each half period. This can lead to large uncontrolled variations of the arm capacitor voltages V_C. A simulation of a three phase MMC with $N = 30$ SM per arm is performed on Matlab/Simscape to illustrates that effect. The 60 capacitor voltages of phase U are given Fig.7. It can be seen that one SM is kept bypassed during the converter operation. At the converter startup, it deviated from other capacitor voltages. Then, it is kept bypassed by RSF during the whole converter operation. Furthermore, high voltage

deviations can be observed. Such instabilities prevent the use of both NLM and RSF algorithm. Next section proposes two new hybrid NLM-PWM modulations that solves the issue highlighted in that section.

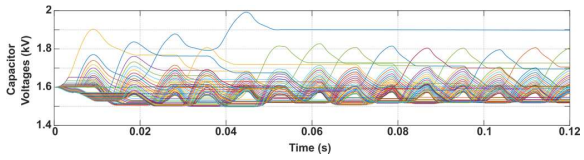

Fig. 7. MMC 60 arm capacitor voltages with NLM and RSF algorithm

III. Novel Hybrid Modulations with Modified Static Carriers and Long Conduction Time

A. Long Conduction Time Pulse Width Modulation

It has been shown in previous section that NLM cannot be used with RSF algorithm due to its staircase behavior. The insertion index must change its sign sufficiently often. That work proposes to add switchings in the NLM waveform. Some references had proposed hybrid modulations with both NLM and PWM characteristics [22][23]. However, when triangular carriers are used, narrow pulses appear, and the output frequency may be unnecessarily increased. This works proposes the generation of two hybrid NLM-PWM waveforms with Modified Static Carriers (MSC). The first modulation proposed in that work is the "Long-Conduction-Time PWM" (LCPWM), given Fig. 8.

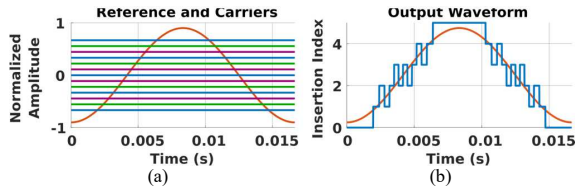

Fig. 8. Proposed "LCPWM": reference and carriers (a), reference and output waveform (b)

Two new sets of carriers (purple and green) are introduced between previous static carriers (blue). The set of principle carrier (blue) proposed for that modulation is generated via a slightly different equation. It produces an output waveform closer to the reference than with previous NLM carrier repartition. The new equation of the lines D_p for the generation of p blue carriers is given in (9).

$$D_p = \frac{2p}{N+1} - 1 \tag{9}$$

The rule for the insertion index generation is sum up in Fig. 9. A set of N blue carriers are generated as in (9). The space between each blue carrier is equal to $2 / (N+1)$. Two more sets of secondary carriers are generated from the previous one by adding respectively a third (green), and two thirds (purple) of that spacing. Then, only M blue carriers are selected depending on the modulation index m, that is, all carriers meeting the condition $-m < D_p < m$. The secondary carrier selection process is the same, but the M^{th} carrier is also suppressed. There are only $M - 1$ carriers in each set of secondary carriers. Finally, each carrier set is compared to the voltage reference. The resulting insertion index is the sum of blue and green comparisons, minus purple comparisons.

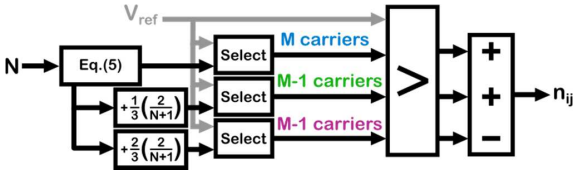

Fig. 9. Carriers and insertion index generation with proposed modulation

The space between carriers is kept constant. This produces an equal repartition between each carrier, maximizing the conduction times, and introduces PWM characteristics in NLM. However, the proposed modulation method generates a high number of switchings. Secondary carriers generate two more switchings at each level of classical NLM. The conduction time of each level is divided by 3, and the switching frequency can be significantly increased. The number of switching N_{sw} per period can be calculated as for NLM. The number of blue carriers N_{carr} is unchanged, and given in (6). The value of p_{max} is obtain as in previous section with the LCPWM blue carrier disposition, and given in (10).

$$p_{max} = \left\lfloor \left(\frac{(N+1)(m+1)}{2} \right) \right\rfloor \tag{10}$$

The number of supplementary switchings N_{sw_sec} produced by secondary carriers depends on the parity of N, the number of submodule, as in (11).

$$\begin{cases} N_{sw\_sec} = 4\,(N_{carr} - 2) & \text{if N even} \\ N_{sw\_sec} = 4\,(N_{carr} - 1) & \text{if N odd} \end{cases} \tag{11}$$

Finally, the number of switchings per period N_{sw} produced by the LCPWM is given in (12).

$$\begin{cases} N_{sw} = 8\,p_{max} - 5N - 8 & \text{if N even} \\ N_{sw} = 8\,p_{max} - 5N - 2 & \text{if N odd} \end{cases} \tag{12}$$

B. Enhanced Long Conduction Time Pulse Width Modulation

Another hybrid modulation is introduced, offering a trade-off between switching frequency and capacitor voltage deviation with RSF. It is the Enhanced Long Conduction Time Pulse Width Modulation (ELCPWM) given in Fig 10. The ELCPWM carrier repartition is based on the previous one, but with "holes" where the secondary carriers (green and purple) are suppressed around the 0 axis. The number of "holes" H can be selected as a trade-off between the capacitor voltage deviation and the switching frequency, as will be showed next section. In the example given Fig 10. the "2-ELCPWM" is presented ($H = 2$).

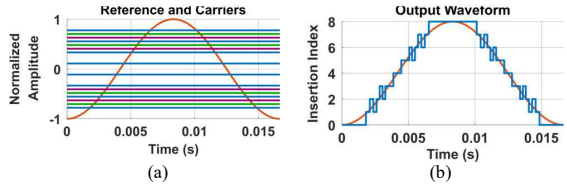

(a) (b)

Fig. 10. Proposed "2-ELCPWM": reference and carriers (a), reference and output waveform (b)

The proposed hybrid waveform exhibits NLM characteristics around the 0 axis. The number of switchings produced by ELCPWM is reduced compared to LCPWM. The secondary carriers around the 0 axis are suppressed with the proposed ELCPWM in order to maximize the conduction times of the proposed modulation, where the sinusoidal reference derivative is maximum. The number of switching per period generated by ELCPWM can be easily calculated as well. The number of switch per period N_{sw} produced by ELCPWM is given in (13). It is reduced by $4H$ compared to previous modulation.

$$\begin{cases} N_{sw} = 8\,p_{max} - 5N - 8 - 4H & \text{if } N \text{ even} \\ N_{sw} = 8\,p_{max} - 5N - 2 - 4H & \text{if } N \text{ odd} \end{cases} \quad (13)$$

In addition to their simplicity of generation and low software cost, the proposed modulations have the advantage of being deterministic. Each conduction time only depends on the reference modulation index. There are no random narrow pulses, unlike with classical PWM methods.

Simulation presented Fig. 7 is performed again in the same conditions with 15-ELCPWM. The results are shown Fig. 11. It can be seen that the voltage balancing is effectively realized by RSF algorithm, and no voltage instabilities can be observed. This is due to the new switchings introduced in the ELCPWM compared to NLM. A detailed simulation is performed next section in order to compare proposed modulations with typical PWM scheme.

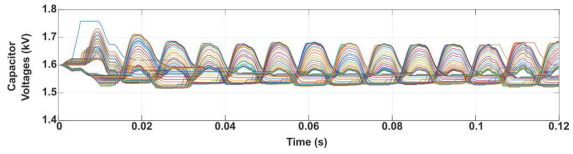

Fig. 11. MMC 60 arm capacitor voltages with 15 - ELCPWM and RSF algorithm

IV. Validation with MATLAB/Simulink Simulation

A Matlab/Simscape simulation of a three-phase MMC allows the comparison of the proposed modulations with a typical PDPWM scheme. The number of submodule of the proposed simulated converter is $N = 30$. The converter delivers power to a grid which voltage is $V_{grid} = 17$ kV, through a link inductor of value $L_{grid} = 19$ mH and a parasitic resistance $R = 1\ \Omega$. The DC bus voltage is $U_{DC} = 48$ kV. The submodule capacitor value is $C = 4.1$ mF and the average capacitor voltage is $V_{Cref} = 1600$ V. The arm inductors have a value of $L_{arm} = 0.5$ mH. The output apparent power is $S = 11.6$ MVA and the power factor is 0.65. The MMC output voltages and currents are shown Fig. 12 for various modulations. The U-phase corresponding 60 capacitor voltages are given Fig. 13. The dark dashed lines give the interval were $V_C \in V_{Cref} \pm 10$ %, which is a common maximum voltage deviation criterion [24]. The modulations compared in that simulation are, from upper to lower, the NLM, the 16 - ELCPWM, the 10 - ELCPWM, the LCPWM and the PDPWM with 6 kHz triangular carriers.

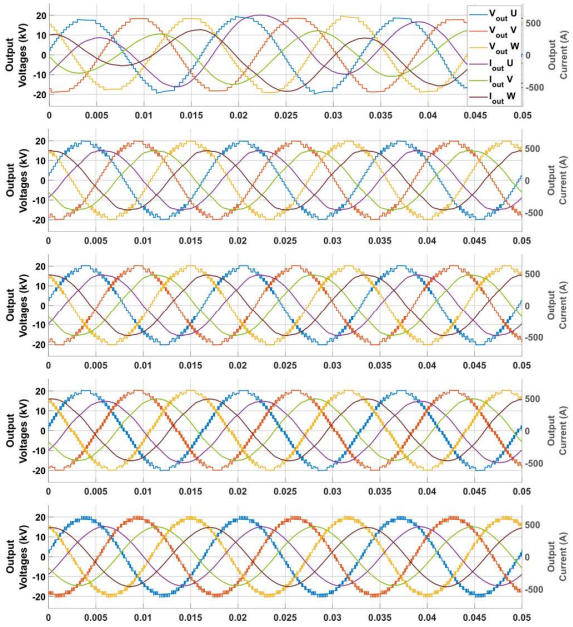

Fig. 12. Three-phase MMC output voltages and currents with various modulations

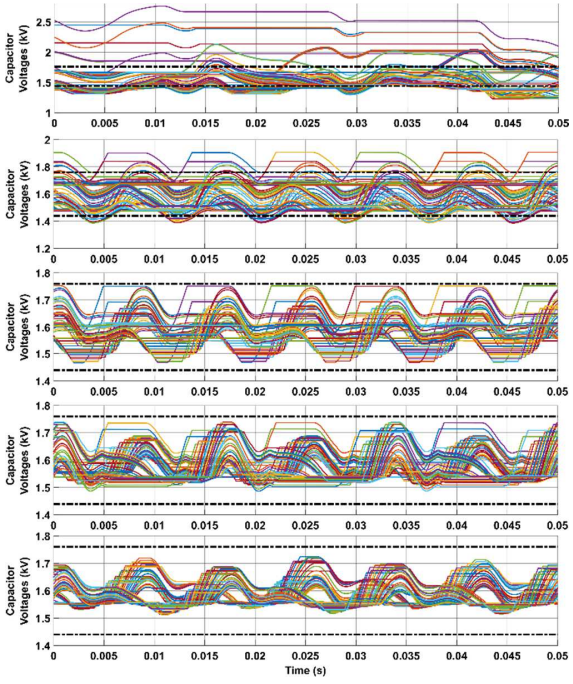

Fig. 13. Three-phase MMC U-phase capacitor voltages with various modulations

The average output switching frequency f_{switch}, the minimum conduction duration t_{min} and the maximum arm voltage spread ΔV_{spread} obtain for each modulation is sum up in Table I. ΔV_{spread} is calculated as the difference between the highest and the lowest capacitor voltage and must ideally be kept under 20% of V_{Cref}, i.e. 320 V. As expected, the NLM modulations generates large and unstable capacitor voltage deviations with RSF. It can be seen that the ENLM offers a highly interesting tradeoff between these 3 characteristics, depending on the number of "Holes" in the waveform. However, the output current is slightly impacted by proposed static carriers based modulations. Further analysis is necessary in order to optimize the carrier repartition proposed in that work to reduce current THD.

TABLE I. MAIN CHARACTERISTICS OF COMPARED MODULATIONS

Modulations	f_{switch}	t_{min}	ΔV_{spread}
NLM	1.5 kHz	210 µs	1526 V
16 - ELCPWM	2.6 kHz	100 µs	519 V
10 - ELCPWM	3.6 kHz	70 µs	283 V
LCPWM	4.7 kHz	60 µs	225 V
PDPWM	6 kHz	< 10 µs	190 V

V. CONCLUSION

The aim of that paper is to propose new hybrid modulation methods based on Nearest Level Modulation with long conduction time. The NLM was studied and generated through static carriers. Such carriers present very simple generation process, based on a unique equation. They do not require much hardware resources contrary to classical triangular or saw-tooth carriers and are thus well suited for converter with high number of level. It has been shown analytically and by simulation that RSF algorithm used together with NLM leads to capacitor voltage instabilities. This is due to the inherent "staircase" waveform produced by NLM. Those considerations lead to the introduction of two based-NLM hybrid modulations compatible with RSF. Both modulations are based on the same set of modified static carriers. A very straightforward scheme is proposed for their generation, ensuring low software cost. The proposed modulation exhibits long and deterministic conduction times. There are no random narrow pulses in the output waveform as with conventional PWM. First, the Long Conduction time PWM is presented. It is perfectly suited to be used with RSF algorithm as it introduces regular capacitor insertions and bypassing compared to NLM. However, its switching frequency is high.

A trade-off is proposed between the switching frequency and the capacitor voltage deviation with RSF algorithm. The Enhanced Long Conduction time PWM is introduced. It is based on the same modified carrier set than LCPWM, but some secondary carriers are suppressed around the 0 axis. This limits the number of switchings of the output waveform but decreases the effectiveness of the voltage sorting. The number of "holes" in the proposed modulation is a tunable parameter. It allows the engineer to adapt the modulation to fulfill the application requirements. An accurate Matlab/Simscape simulation of a three phase MMC is performed in order to compare the proposed modulations with a typical Phase Disposition PWM scheme. The ELCPWM offers best tradeoff between capacitor voltage balancing and switching frequency. Furthermore, no narrow pulses are generated due to the proposed static carriers. Such modulation scheme is very promising for high power, high number of submodule MMC. The implementation of the proposed modulations on real MMC will be thoroughly studied in future works.

REFERENCES

[1] Lesnicar, A.; Marquardt, R. An innovative modular multilevel converter topology suitable for a wide power range. 2003 IEEE Bol. PowerTech - Conf. Proc. 2003, 3, 272–277, doi:10.1109/PTC.2003.1304403.

[2] Vijeh, M.; Rezanejad, M.; Samadaei, E.; Bertilsson, K. A General Review of Multilevel Inverters Based on Main Submodules: Structural Point of View. IEEE Trans. Power Electron. 2019, 34, 9479–9502, doi:10.1109/TPEL.2018.2890649.

[3] Tian, Y.; Wickramasinghe, H.R.; Li, Z.; Konstantinou, G. Modular Multilevel Converter Sub-modules for HVDC Applications. 2020 IEEE 9th Int. Power Electron. Motion Control Conf. IPEMC 2020 ECCE Asia 2020, 1510–1515, doi:10.1109/IPEMC-ECCEAsia48364.2020.9368019.

[4] Zhang, L.; Qin, J.; Shi, D.; Wang, Z. Improved equivalent circuit model of MMC and influence analysis of simulation time step. IET Power Electron. 2020, 13, 2212–2221, doi:10.1049/iet-pel.2019.1043.

[5] Liu, M.; Li, Z.; Yang, X. A universal mathematical model of modular multilevel converter with half-bridge. Energies 2020, 13, 1–18, doi:10.3390/en13174464.

[6] Nguyen, M.H.; Kwak, S. Nearest-Level Control Method with Improved Output Quality for Modular Multilevel Converters. IEEE Access 2020, 8, 110237–110250, doi:10.1109/ACCESS.2020.3001587.

[7] Ilves, K.; Member, S.; Norrga, S.; Harnefors, L.; Member, S. On Energy Storage Requirements in Modular Multilevel Converters. IEEE Trans. Power Electron. 2014, 29, 77–88, doi:10.1109/TPEL.2013.2254129.

[8] Seleme, S.I.; Grégoire, L.A.; Cousineau, M.; Ladoux, P. Modular control with carrier auto-interleaving and capacitor-voltage balancing for MMCs. IET Power Electron. 2019, 12, 817–828, doi:10.1049/iet-pel.2018.5096.

[9] Xia, B.; Li, Y.; Li, Z.; Konstantinou, G.; Xu, F.; Gao, F.; Wang, P. Decentralized Control Method for Modular Multilevel Converters. IEEE Trans. Power Electron. 2019, 34, 5117–5130, doi:10.1109/TPEL.2018.2866258.

[10] Guo, P.; Li, Y.; He, Z.; Yue, Y.; Xu, Q.; Luo, A. Multistage Model Predictive Control for Modular Multilevel Converter. Proc. - 2018 IEEE Int. Power Electron. Appl. Conf. Expo. PEAC 2018 2018, doi:10.1109/PEAC.2018.8590344.

[11] Liu, M.; Li, Z.; Yang, X. Tracking control of modular multilevel converter based on linear matrix inequality without coordinate transformation. Energies 2020, 13, 1–15, doi:10.3390/en13081978.

[12] Hassanpoor, A.; Ängquist, L.; Norrga, S.; Ilves, K.; Nee, H.P. Tolerance band modulation methods for modular multilevel converters. IEEE Trans. Power Electron. 2015, 30, 311–326, doi:10.1109/TPEL.2014.2305114.

[13] Hassanpoor, A.; Roostaei, A.; Norrga, S.; Lindgren, M. Optimization-based cell selection method for grid-connected modular multilevel converters. IEEE Trans. Power Electron. 2016, 31, 2780–2790, doi:10.1109/TPEL.2015.2448573.

[14] Choudhury, A.; Shimada, T.; Kanouda, A.; Mabuchi, Y. Reduced switching loss based cell capacitor voltage balancing strategy for MMC. 9th IEEE Int. Conf. Power Electron. Drives Energy Syst. PEDES 2020 2020, doi:10.1109/PEDES49360.2020.9379800.

[15] Tu, Q.; Xu, Z.; Xu, L. Reduced Switching-frequency modulation and circulating current suppression for modular multilevel converters. IEEE Trans. Power Deliv. 2011, 26, 2009–2017, doi:10.1109/TPWRD.2011.2115258.

[16] Hasan, N.S.; Rosmin, N.; Osman, D.A.A.; Musta'amal Jamal, A.H. Reviews on multilevel converter and modulation techniques. Renew. Sustain. Energy Rev. 2017, 80, 163–174, doi:10.1016/j.rser.2017.05.163.

[17] Ali, S.; Soomro, J.B.; Mughal, M.; Chachar, F.A.; Bukhari, S.S.H.; Ro, J.S. Power Quality Improvement in HVDC MMC with Modified

Nearest Level Control in Real-Time HIL Based Setup. IEEE Access 2020, 8, doi:10.1109/ACCESS.2020.3043811.

[18] Chen, Y.; Cui, Y.; Tao, Y.; Kang, Y.; Wei, X.; Wang, X. High-fundamental-frequency modulation for the DC-DC modular multilevel converter (MMC) with low switching frequency and predicted-based voltage balance strategy. IEEE Transp. Electrif. Conf. Expo, ITEC Asia-Pacific 2014 - Conf. Proc. 2014.

[19] Guan, B.; Wang, C. A narrow pulse compensation method for neutral-point-clamped three-level converters considering neutral-point balance. 9th Int. Conf. Power Electron. - ECCE Asia "Green World with Power Electron. ICPE 2015-ECCE Asia 2015, 2770–2775.

[20] Mu, J.; He, Z.; Xu, Y.; Zhang, X.; Long, Y. The Generation Mechanism and Elimination Strategy of Narrow- And Error-Pulse for Cascaded H-Bridge NL-PWM Modulation. IEEE Access 2021, 9, 52860–52871, doi:10.1109/ACCESS.2021.3070661.

[21] Corentin, D.; Nicolas, G.; Jean-Christophe, O.; Frederic, P. Modular Multilevel Converter with Distributed Galvanic Isolation: A Decentralized Voltage Balancing Algorithm with Smart Gate Drivers. 2020 22nd Eur. Conf. Power Electron. Appl. EPE 2020 ECCE Eur. 2020, 1, 1–10, doi:10.23919/EPE20ECCEEurope43536.2020.9215896.

[22] MOHAMMAD IRFAN, S.; ADIL, S.; SHOEB AZAM, F.; MOHD, T.; MOHAMMAD, F.; ABDUL, R.B.; BASEM, A. A Hybrid Nearest Level Combined With PWM Control Strategy: Analysis and Implementation on Cascaded H-Bridge Multilevel Inverter and its Fault Tolerant Topology. IEEE Access 2021, 9, 44266–44282, doi:10.1109/ACCESS.2021.3058136.

[23] De Simone, D.; Tricoli, P.; D'Arco, S.; Piegari, L. Windowed PWM: A Configurable Modulation Scheme for Modular Multilevel Converter-Based Traction Drives. IEEE Trans. Power Electron. 2020, 35, 9729–9738, doi:10.1109/TPEL.2020.2969375.

[24] Sharifabadi, K.; Harnefors, L.; Nee, H.-P.; Norrga, S.; Teodorescu, R. Design, Control and Application of Modular Multilevel Converters for HVDC Transmission Systems; Wiley - IEEE Press, 2016; ISBN 978-1-118-85156-2.